Model for the temperature dependence of the quasiparticle interference pattern in the measured scanning tunneling spectra of underdoped cuprate superconductors

Dan Wulin,[1] Yan He,[1] Chih-Chun Chien,[1] Dirk K. Morr,[1,2] and K. Levin[1]
[1]*James Frank Institute and Department of Physics, University of Chicago, Chicago, Illinois 60637, USA*
[2]*Department of Physics, University of Illinois at Chicago, Chicago, Illinois 60607, USA*
(Received 24 August 2009; revised manuscript received 2 September 2009; published 6 October 2009)

In this paper we explore the behavior of the quasiparticle interference (QPI) pattern of scanning tunneling microscopy as a function of temperature T, for moderately underdoped cuprates. After ensuring a minimal consistency with angle-resolved photoemission spectroscopy, we find that the QPI pattern is profoundly sensitive to quasiparticle coherence and that it manifests two energy-gap scales. In particular, we find that the superconducting QPI pattern vanishes at the same temperature as that at which the Fermi arcs appear. Experimental support for this conclusion comes from the observation of a nearly dispersionless QPI pattern which has been observed to appear above T_c in moderately underdoped cuprates. To illustrate the important two energy scale physics we present predictions of the QPI-inferred energy gaps as a function of T for future experiments on moderately underdoped cuprates. This defines the so-called "Bogoliubov arcs," which we find have an extinction point controlled by the size of the superconducting order parameter. This extinction, thus, seems unrelated to the magnetic zone boundary. Moreover, the calculated Bogoliubov arcs persist across the full nodal region, as might be expected, since that is where the superconductivity is thought to be dominant. A second larger energy scale is implied from extrapolation to the antinodes, presuming a simple d-wave shape and that the temperatures are not too close to T_c. This corresponds to the pseudogap energy scale in the literature.

DOI: 10.1103/PhysRevB.80.134504 PACS number(s): 74.25.Jb, 74.20.−z, 74.72.−h

I. INTRODUCTION

Recently, attention in the field of high-temperature superconductivity has turned to characterizing the superconducting (sc) phase in the underdoped regime. This phase necessarily differs from that of a conventional d-wave superconductor because components of the gap smoothly evolve through T_c. This leads to a normal-state gap or pseudogap above T_c. Owing to this fact, and unlike a BCS superconductor where the order parameter and the excitation gap are identical, there are very few ways to directly probe the energy gap tied to the superconducting order parameter.

Within the moderately underdoped samples, which we consider throughout this paper, recent angle-resolved photoemission spectroscopy (ARPES) experiments have reported[1,2] important signatures of superconducting order. Passing through T_c from above, Fermi arcs around the d-wave nodes rapidly collapse[2] to form point nodes. It was argued that, within the superconducting phase, the temperature dependence of the nodal gap has finally provided[1] "a direct and unambiguous observation of a single-particle gap tied to the superconducting transition." A complementary and equally valuable probe is scanning tunneling microscopy (STM) and the related quasiparticle interference (QPI) spectroscopy.[3–7] While this probe, like ARPES, is generally not phase sensitive, a controversy has arisen as to whether these techniques can, as argued experimentally,[4,6] or cannot, as summarized theoretically,[5,8] distinguish coherent superconducting order from pseudogap behavior.

The objective of this paper is to provide a resolution to this controversy by studying the temperature evolution of the QPI pattern observed in STM experiments from the superconducting ground state into the pseudogap phase at $T \gtrsim T_c$. We employ a *microscopically derived* preformed pair theory[9] that accounts[10] for all of the complex momentum and temperature dependence of the ARPES spectral gap that is described above. STM has been extensively used to probe the local density of states (LDOS) of cuprate superconductors, associated with a single impurity. The resulting quasiparticle interference pattern is associated with energy-dependent modulations[3–5,11] in the LDOS that reflect electronic structure. In the superconducting state, the dispersive QPI (Refs. 12 and 13) or octet features arise from transitions which are associated with the set of wave vectors that connect (eight) tips on banana-shaped equal-energy contours. The QPI peaks in momentum space must satisfy certain consistency conditions due to the d-wave symmetry of the gap.

A central result of our study is that, once compatibility with ARPES experiments is incorporated, the observation of the so-called "octet model" QPI (Refs. 12 and 14) (called Bogoliubov QPI or B-QPI) is a direct signature of *coherent* superconducting order: sets of consistent octet model vectors can only be found for energies less than the superconducting order-parameter energy scale. In a related fashion, B-QPI does not persist above T_c, where the order parameter vanishes. In this way, QPI patterns, like the behavior of the penetration depth and Andreev scattering, are found to be sensitive to superconducting coherence. We stress that this behavior is associated with the moderately underdoped cuprates and the counterpart for the highly underdoped regime, where ARPES is also more complicated,[15] may be less straightforward.[16]

II. THEORY BACKGROUND

Our preformed pair theory,[9,10] which has also been successfully applied to the ultracold atoms, is based on BCS-

Bose Einstein condensation crossover theory. We focus on a stronger than BCS attractive interaction which is thought to be present because of the anomalously short coherence length. The ground state is the usual BCS state with a self-consistently determined chemical potential. As outlined elsewhere,[9] we solve coupled equations for the fermionic and pair propagators. In the pseudogap region below T^*, there are preformed pairs that become noncondensed pair excitations of the condensate below T_c. For $T<T_c$, both noncondensed and condensed pairs coexist but there is a *gradual* conversion from noncondensed to condensed pairs as temperature is decreased, leading to the conventional BCS ground state as $T\to 0$.

The pair propagator is related to the t matrix, $t(Q)=t_{sc}(Q)+t_{pg}(Q)$ (with Q defined as a four vector), where $t_{sc}(Q)\equiv -\frac{\Delta_{sc}^2}{T}\delta(Q)$ and $t_{pg}(Q)$ represent the contribution to the t matrix from condensed and noncondensed pairs, respectively. The noncondensed pair contribution $t_{pg}(Q)$ is obtained from a particle-particle t matrix[10] that includes one dressed (G) and one bare (G_0) Green's function.[17] The contribution of the noncondensed pairs to the full self-energy $\Sigma(K)\equiv\Sigma_Q t(Q)G_0(Q-K)\varphi^2_{\mathbf{k}-\mathbf{q}/2}$ can be well approximated in terms of a pseudogap parameter $\Delta_{pg}(\mathbf{k})$ because $t_{pg}(Q)$ is strongly peaked at small Q for T slightly above T_c and $T\leq T_c$. Thus, $\Sigma(\mathbf{k},\omega)$ consists[18] of two terms (with $\omega+i\delta$, $\delta=0^+$ implicitly assumed)

$$\Sigma(\mathbf{k},\omega)=\Sigma_{sc}(\mathbf{k},\omega)+\Sigma_{pg}(\mathbf{k},\omega)=\frac{\Delta_{sc}^2(\mathbf{k})}{\omega+\xi_{\mathbf{k}}}+\frac{\Delta_{pg}^2(\mathbf{k})}{\omega+\xi_{\mathbf{k}}+i\gamma}. \tag{1}$$

The two gap parameters, $\Delta_{sc}(\mathbf{k})=\Delta_{sc}\varphi_{\mathbf{k}}$ and $\Delta_{pg}(\mathbf{k})=\Delta_{pg}\varphi_{\mathbf{k}}$, correspond to the sc order parameter and the finite momentum pair gap (pg). The factor $\varphi_{\mathbf{k}}=[\cos(k_x)-\cos(k_y)]/2$ ensures d-wave symmetry. The effective gap which appears in the Bogoliubov quasiparticle dispersion is $\Delta(\mathbf{k},T)=\Delta(T)\varphi_{\mathbf{k}}$ with $\Delta(T)\equiv\sqrt{\Delta_{sc}^2(T)+\Delta_{pg}^2(T)}$. We define the ordered phase through the nonvanishing superfluid density, ρ_s. Microscopic calculations[19] based on Ward identities have established that $\rho_s\propto\Delta_{sc}^2$ as expected. Thus the ordered phase corresponds to $\Delta_{sc}\neq 0$.

Similarly, the damping γ distinguishes the noncondensed pairs from the condensate, as was addressed microscopically in earlier work.[20] There it was numerically shown that the broadened BCS self-energy models the present form for the self-energy, Σ_{pg} with high accuracy. Had we used a different form for the t matrix, other than that associated[17] with BCS theory, this would not be the case.[20] The parameters Δ_{pg} and γ could be extracted from this procedure. However, since the calculations were done for the s-wave case only, we necessarily treat γ phenomenologically here. We present the simplest approximation[10] of our microscopic theory in order to make our calculations more accessible: (i) To reasonable accuracy,[9] $\Delta(T)$ can be found from the BCS gap equation. (ii) Moreover, we approximate[10] $\Delta_{pg}(T)=\Delta(T)(T/T_c)^{3/4}$ for $T\leq T_c$ and $\Delta_{pg}(T)=\Delta(T)$ for $T>T_c$.

The link between ARPES and STM experiments both *below* and *above* T_c is based on the common spectral function $A(\mathbf{k},\omega)=-\mathrm{Im}\,G(\mathbf{k},\omega)/\pi$. The single adjusted parameter γ is constrained through measurements of the Fermi arc size in ARPES. We find the presence of a perceptible Fermi arc (with length $\gtrsim 10\%$ of the Fermi surface) requires[10,21] that $\gamma(T_c)/\Delta(T_c)>0.2$. We have importantly determined that the behavior of QPI that we report in this paper is robust for the same regime, $\gamma(T_c)/\Delta(T_c)>0.2$. Specifically, to account for a Fermi arc of about 20% of the length of the Fermi surface we take[22] $\gamma(T_c)\approx 0.5\Delta_{pg}(T_c)$. *We stress our results are not particularly sensitive to the detailed T* dependence of γ, which, for the present purposes, could have been ignored. For numerical regularization purposes we set $\delta=0.01\Delta(T_c)$.

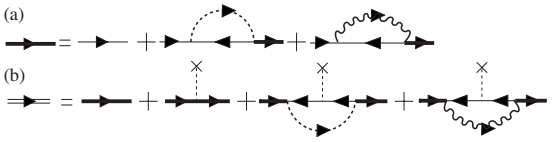

FIG. 1. Full Green's function in (a) the clean case (thick solid line) and (b) in the presence of an impurity (double thin lines) to lowest order in U_0, the impurity strength. A thin line represents the noninteracting normal-state Green's function $G_0=(\omega-\xi_{\mathbf{k}})^{-1}$, and the dotted and wavy lines represent the t matrices t_{sc} and t_{pg}, respectively. Panels (a) and (b) are the basis for our ARPES and QPI analysis.

The full Green's function is $G^{-1}(\mathbf{k},\omega)=\omega-\xi_{\mathbf{k}}-\Sigma(\mathbf{k},\omega)$ [see Fig. 1(a)] and the band structure and other parameters are standard.[23] In the presence of a nonmagnetic impurity, the diagrams contributing to the full Green's function up to first order in the impurity strength U_0 are shown in Fig. 1(b). For a single pointlike impurity, the Fourier transform of the first-order correction to the LDOS is given by

$$\delta n(\mathbf{q},\omega)=-\frac{U_0}{\pi}\mathrm{Im}\left\{\int\frac{d^2k}{(2\pi)^2}[G(\mathbf{k},\omega)G(\mathbf{k}+\mathbf{q},\omega)-F_{sc}(\mathbf{k},\omega)F_{sc}(\mathbf{k}+\mathbf{q},\omega)-F_{pg}(\mathbf{k},\omega)F_{pg}(\mathbf{k}+\mathbf{q},\omega)]\right\}, \tag{2}$$

where

$$F_{sc}(\mathbf{K})\equiv-\frac{\Delta_{sc}(\mathbf{k})G(\mathbf{K})}{\omega+\xi_{\mathbf{k}}};\quad F_{pg}(\mathbf{K})\equiv-\frac{\Delta_{pg}(\mathbf{k})G(\mathbf{K})}{\omega+\xi_{\mathbf{k}}+i\gamma}$$

and $\mathbf{K}=(\mathbf{k},\omega)$. There are two types of FF terms: the usual one which depends on F_{sc} associated with the sc condensate[14] and an additional term (involving F_{pg}) represented by the last diagram on the right-hand side of Fig. 1(b); this reflects the contribution of preformed (or noncondensed) pairs. Importantly, this term that has not appeared in previous work is required for microscopic consistency.

III. RESULTS AND DISCUSSION

We present the evolution of the QPI pattern with temperature in Fig. 2 and show $|\delta n(\mathbf{q},\omega)|$ for $\omega=-10$ meV and several temperatures, $T/T_c=0.1$, 0.5, 0.9, and 1.1 in panels (a)–(d). Within the octet model picture,[12,14] δn in a d-wave superconductor is dominated by the seven vectors [four of

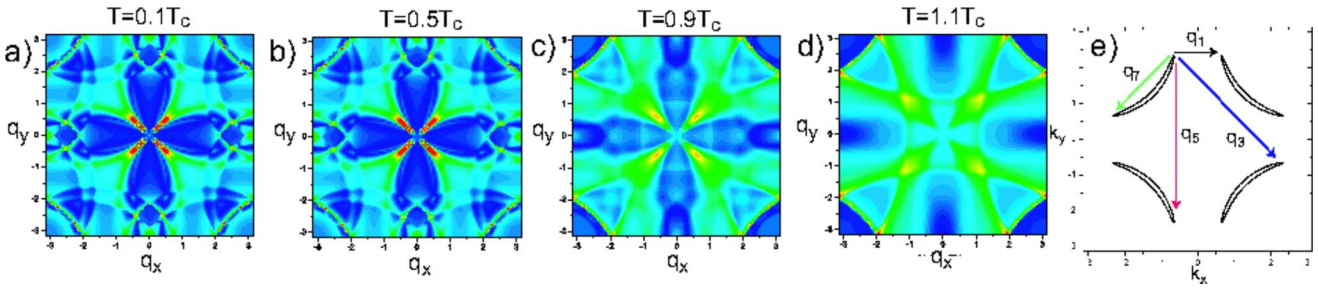

FIG. 2. (Color online) [(a)–(d)] Intensity plot of $|\delta n(\mathbf{q},\omega)|$ at $\omega=-10$ meV for increasing T. From left to right: $T/T_c=0.1$, 0.5, 0.9, and 1.1. (e) Equal-energy contours and the dispersive octet vectors that describe the dispersive B-QPI vectors in the superconducting phase. The unit of wave vectors is the inverse lattice constant.

them are illustrated in Fig. 2(e)]. We will find that in addition to a characteristic dispersion in which the octet vectors satisfy specific consistency conditions, the peak intensity has a strong dependence on temperature. As T_c is approached and Δ_{sc} vanishes, the octet model illustrated in Fig. 2(e) fails. While the QPI pattern remains relatively unchanged up to $T=0.5T_c$, the peak intensity begins to rapidly drop above this temperature. This reflects that gradual conversion of condensed pairs to noncondensed pairs with increasing temperature and that $\Delta_{pg}(T)$ is suppressed relative to $\Delta_{sc}(T)$ at lower temperatures.

At $T/T_c=0.9$ the characteristic (superconducting) QPI pattern becomes smeared out (due to the rapid rise in the number of noncondensed pairs) and the octet peaks are found to vanish above T_c. Note that the QPI pattern above T_c is also distinctively different from that of a gapless normal phase.[5,14] The presence of noncondensed pairs below T_c and preformed pairs above T_c also guarantees that the QPI pattern evolves smoothly (as in a second-order phase transition) through T_c.

In order to elucidate the temperature dependence of the QPI pattern more quantitatively, we plot in Fig. 3 $|\delta n(\mathbf{q},\omega)|$ as a function of q along the horizontal ($q_y=0$) and diagonal ($q_y=q_x$) directions for $\omega=-10$ meV. The insets of Figs. 3(a) and 3(b) show the temperature dependence of the peak intensity for the dispersing vectors. In agreement with the above discussion, the peak intensities decrease significantly for $T>0.5T_c$. At $T\approx T_c$, the peaks associated with the dispersing branches q_1, q_3, q_5, and q_7 all vanish (the peaks associated with q_1 and q_7 merge into the background and thus should not be identified as distinctive individual peaks). These insets show that the B-QPI pattern is uniquely associated with superconducting coherence; as the coherent pairs are converted to pairs with finite lifetime, the QPI peaks are strongly damped and octet signature vanishes. This strong signature of T_c in QPI is correlated with its counterpart in ARPES (Refs. 1 and 2) for moderately underdoped systems because the same inverse lifetime γ that generates Fermi arcs is responsible for the destruction of octet peaks at T_c.

We turn now to detailed plots of the QPI peak dispersion that reinforce these conclusions. The dispersive behavior vanishes in the normal state, as is consistent with experiment.[6] This is shown in Figs. 4(a)–4(j) where $|\delta n(\mathbf{q},\omega)|$ is plotted as a function of ω and momentum along the diagonal and horizontal directions. From these two rows the presence and consistency of dispersive octet vectors can be verified. In the diagonal cut at $T=0.1T_c$ and at low frequencies and momentum $q\approx 0$, we identify the octet vector q_7 [see Fig. 4(a)] while the peak at momentum $q\approx 2.5$ corresponds to q_3. In the horizontal cut, we identify the dispersing q_1 and q_5 branches, which for $\omega\to 0$ merge into a single point, $q\approx 2.55$. The momenta q_1, q_3, q_5, and q_7 satisfy the constraints of the octet model for sufficiently low ω. We identify several nondispersive features in the B-QPI pattern that reflect the normal state. It is not clear to what extent the nondispersive features seen experimentally[6] above T_c are present here.

In the diagonal cuts Figs. 4(a)–4(d), a slowly dispersing feature emerges at positive(negative) frequencies near $q_x=1.2(1.0)$. This corresponds to the normal-state peak in Fig. 4(e) that is present for all energies. A similar feature is observable in the horizontal cuts Figs. 4(f)–4(i) for large frequencies and $q_x\approx 1.1$. In contrast to the strongly dispersive features, the intensity of these branches decreases only slightly through T_c and persists to higher temperatures since

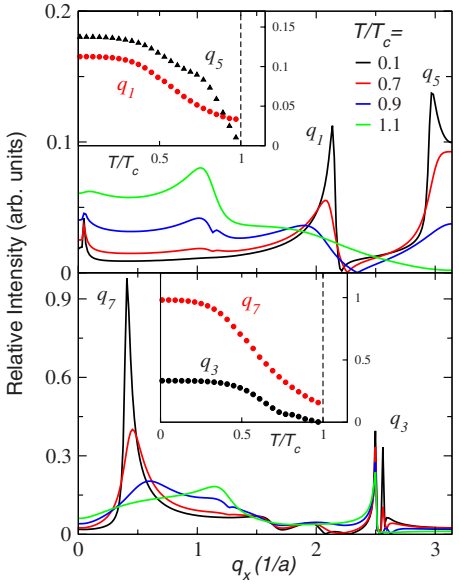

FIG. 3. (Color online) One dimensional cuts for fixed frequency $\omega=-10$ meV in the (a) horizontal and (b) diagonal directions. Intensities of peaks fall off rapidly as Cooper pairs lose coherence. Insets specify temperature dependence of q-vector intensity. All octet peaks disappear at and above T_c, although there is a finite background for q_1 and q_7.

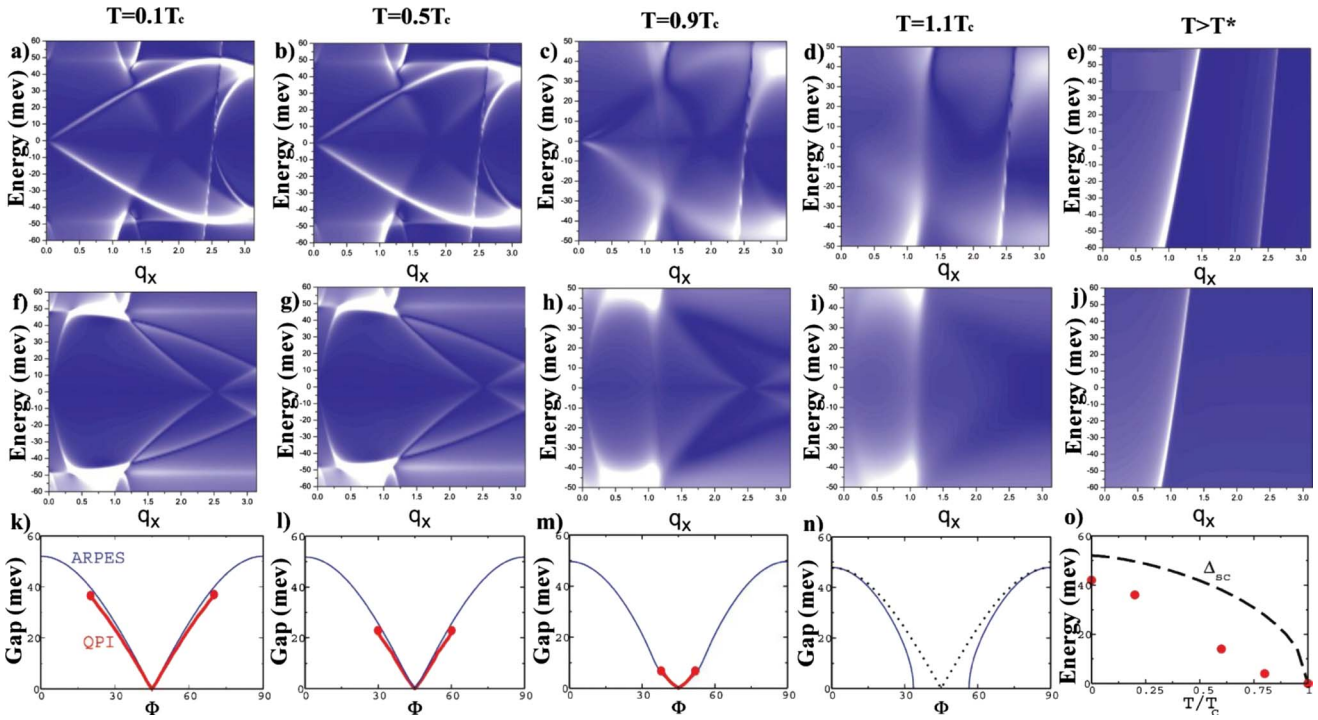

FIG. 4. (Color online) First (second) row shows diagonal (horizontal) cuts along $q_x=q_y$ ($q_y=0$) at $\omega=-10$ meV for increasing T from left to right $T/T_c=0.1$, 0.5, 0.9, and 1.1. The last row plots the B-QPI gap (thick red lines) at the same temperatures inferred from pairs of octet vectors along the horizontal and diagonal directions, compared with the ARPES gap (thin blue lines). When the inconsistency between the inferred points on the Fermi surface, k_x and k_y, exceeds 5% the inversion procedure is terminated. The last figure [panel (o)] on the right shows the temperature dependence of the energy where the octet model breaks down (red dots), which falls with temperature, like the order parameter (black dashed line). The dotted line in the adjacent figure [panel (n)] represents the simple d-wave gap shape. It is clear that, as in experiment (Ref. 1) the ARPES gap varies smoothly across T_c as in a second-order phase transition.

they are present in the normal state. Note that due to Umklapp scattering, the q_5 branch is reflected back into the first Brillouin zone for frequencies $|\omega|>13$ meV.[14] For $\omega\approx\Delta$, the two branches merge into a single one that for even larger frequencies again becomes nearly nondispersive, as is a expected from the normal-state QPI pattern.

In the last row of Fig. 4, we probe the effects of superconducting coherence in a way that is strictly confined to the $T\leq T_c$ state. Here we display the gap obtained for a given temperature from the B-QPI pattern dispersion shown in the first two rows using the octet model inversion procedure.[4] For a given energy ω, the inversion procedure yields points on the Fermi surface, k_x and k_y, such that $\Delta(k_x,k_y)=\omega$. Each row was used to generate an independent set of points and we take a maximal 5% disagreement between these two sets as a necessary condition for the observation of B-QPI. The ARPES-derived gap[10] is plotted for comparison. The ARPES and B-QPI gaps agree well for energies where the horizontal and diagonal cuts yield consistent k_x and k_y points. In particular, at low temperatures and for frequencies $\omega>0.8\Delta_{sc}$, we find the two sets of Fermi-surface points extracted from the octet vectors differ by more than 5%. At higher temperatures this occurs at increasingly smaller frequencies with respect to the size of Δ_{sc}. This leads to a frequency cutoff in the inversion procedure which is plotted in the rightmost panel of the bottom row as a function of temperature, where it tracks the superconducting order parameter Δ_{sc}. One can see from the panel at $T/T_c=0.9$ that Fermi arc physics is also apparent below T_c in the rounding of the QPI-inferred gap at low energy. Both gaps extrapolate at the antinodes to approximately 50 meV$\approx\Delta(T)$. We also observe that below $0.8T_c$ the extracted B-QPI gap follows a d-wave shape and thus the total gap (to be distinguished from the order parameter) can be inferred by extrapolating the B-QPI gap to the antinodes and it is almost independent of temperature.

The segments of **k** space where B-QPI inversion is possible correspond to the so-called[4] "Bogoliubov arcs" whose end points are associated with "**k**-space extinction." This in turn appears unrelated to either the Fermi arcs or the magnetic zone boundary, as claimed elsewhere.[4] [It has moreover been speculated that the arcs and magnetic zone boundary are connected, although this does not appear to be the case in general[15]]. *Rather we find that the Bogoliubov arcs are controlled by the size of the superconducting* Δ_{sc} order parameter. This is consistent with our discussion of Fig. 2, which observed that B-QPI vanishes as $T\rightarrow T_c$ and $\Delta_{sc}\rightarrow 0$.

While our results for $T\ll T_c$ are in agreement with those of earlier studies,[12,14] our results for temperatures above T_c differ in several important respects from previous work.[5,8] In contrast to the pseudogap theory proposed in Ref. 8, we incorporate the presence of Fermi arcs in ARPES above T_c. This may explain why the pseudogap QPI pattern of Ref. 8 is qualitatively similar to that of the sc state. On the other hand, in Ref. 5 the Fermi arcs were incorporated but under the presumption that the gap parameters entering the calculation of the QPI pattern and the spectral gaps observed in ARPES

experiments were equivalent. The resultant QPI pattern disagreed with the experimental results and it was therefore suggested that the pseudogap phase may be unrelated to precursor superconductivity. In contrast, we argue in our preformed pair scenario that, while the same formalism must be used to address ARPES and STM experiments (as in Fig. 1), the ARPES spectral gap should not be directly employed in the calculations of the QPI pattern.

IV. CONCLUSION

In summary, in our QPI studies two distinct scales appear: the total gap Δ as inferred (by extrapolating the B-QPI gap to the antinodes presuming a d-wave shape) and Δ_{sc}, the frequency at which B-QPI breaks down. As in experiment[1,4] we find that $\Delta_{sc}(T)$, which vanishes at T_c, is more influential in the nodal regime and we are able to deduce this parameter from the "**k**-space extinction" of the QPI-inferred gap. By contrast Δ is roughly T independent. A key difference with Ref. 4 is that we find the inversion procedure works well even down to the precise nodal point. The failure of this procedure when experimentally implemented near the nodes has not been understood.

An important feature of the present theory is its unique ability to address the ordered phase at general T in the presence of a pseudogap. Other theories are confined to $T \approx 0$ or $T > T_c$. It is important but difficult for theorists to find ways to help identify the presence of superconducting order because of the competing presence of the pseudogap. We have shown that the frequency cutoff of the B-QPI gives such a method. We have found an important correlation which makes our predictions very robust. The condition on $\gamma(T_c)$ for the appearance of perceptible Fermi arcs in photoemission is essentially the same as the condition for the disappearance of octet peaks in the normal state.

In heavily underdoped cuprates (not considered here) there have been recent observations[16] of a small contribution to B-QPI in the near vicinity but above T_c. This may reflect the fact that in ARPES experiments for these stoichiometries, Fermi arcs are not present[15] until substantially above the nominal T_c. For these more metallurgically complex cuprates near the insulating phase, more detailed experiments and theory are needed to probe the correlations between B-QPI and ARPES. We end by noting that in retrospect our conclusion that B-QPI disappears with the appearance of Fermi arcs makes sense physically since it is difficult to see how the precise octet vectors will survive in the presence of these arcs.

ACKNOWLEDGMENTS

This work was supported by NSF under Grant No. PHY-0555325, NSF-MRSEC under Grant No. DMR-0213745, and U.S. Department of Energy under Award No. DE-FG02-05ER46225 (D.M.). We thank J.C. Davis, J. Lee, and A. Yazdani for helpful discussions.

[1] W. S. Lee, I. M. Vishik, K. Tanaka, D. H. Lu, T. Sasagawa, N. Nagaosa, T. P. Devereaux, Z. Hussain, and Z. X. Shen, Nature (London) **450**, 81 (2007).
[2] A. Kanigel, U. Chatterjee, M. Randeria, M. R. Norman, S. Souma, M. Shi, Z. Z. Li, H. Raffy, and J. C. Campuzano, Phys. Rev. Lett. **99**, 157001 (2007).
[3] K. K. Gomes, A. Pasupathy, A. N. Pushp, S. Ono, Y. Ando, and A. Yazdani, Nature (London) **447**, 569 (2007).
[4] Y. Kohsaka, C. Taylor, P. Wahl, A. Schmidt, J. Lee, K. Fujita, J. Alldredge, K. McElroy, J. Lee, H. Eisaki, S. Uchida, D.-H. Lee, and J. C. Davis, Nature (London) **454**, 1072 (2008).
[5] S. Misra, M. Vershinin, P. Phillips, and A. Yazdani, Phys. Rev. B **70**, 220503(R) (2004).
[6] M. Vershinin, S. Misra, S. Ono, Y. Abe, A. Yoichi, and A. Yazdani, Science **303**, 1995 (2004).
[7] A. Pushp, C. V. Parker, A. N. Pasupathy, K. K. Gomes, S. Ono, J. Wen, Z. Xu, G. Gu, and A. Yazdani, Science **324**, 1689 (2009).
[8] T. Pereg-Barnea and M. Franz, Phys. Rev. B **68**, 180506(R) (2003).
[9] Q. J. Chen, J. Stajic, S. N. Tan, and K. Levin, Phys. Rep. **412**, 1 (2005).
[10] Q. J. Chen and K. Levin, Phys. Rev. B **78**, 020513(R) (2008); C. C. Chien, Y. He, Q. J. Chen, and K. Levin, *ibid.* **79**, 214527 (2009).
[11] A. Pasupathy, A. Pushp, K. Gomes, C. Parker, J. Wen, Z. Zu, G. Gu, S. Ono, Y. Ando, and A. Yazdani, Science **320**, 196 (2008).
[12] Q.-H. Wang and D.-H. Lee, Phys. Rev. B **67**, 020511(R) (2003).
[13] J. Hoffman, K. McElroy, D.-H. Lee, K. Lang, H. Eisaki, S. Uchida, and J. Davis, Science **297**, 1148 (2002).
[14] L. Capriotti, D. J. Scalapino, and R. D. Sedgewick, Phys. Rev. B **68**, 014508 (2003).
[15] T. Yoshida, M. Hashimoto, S. Ideta, A. Fujimori, K. Tanaka, N. Mannella, Z. Hussain, Z. X. Shen, M. Kubota, K. Ono, Seiki Komiya, Yoichi Ando, H. Eisaki, and S. Uchida, Phys. Rev. Lett. **103**, 037004 (2009).
[16] J. Lee, K. Fujita, A. R. Schmidt, C. K. Kim, H. Eisaki, S. Uchida, and J. C. Davis, Science **325**, 1099 (2009).
[17] L. P. Kadanoff and P. C. Martin, Phys. Rev. **124**, 670 (1961).
[18] Q. J. Chen, K. Levin, and I. Kosztin, Phys. Rev. B **63**, 184519 (2001).
[19] Q. J. Chen, I. Kosztin, B. Jankó, and K. Levin, Phys. Rev. Lett. **81**, 4708 (1998).
[20] J. Maly, B. Jankó, and K. Levin, Phys. Rev. B **59**, 1354 (1999); Physica C **321**, 113 (1999).
[21] A. V. Chubukov, M. R. Norman, A. J. Millis, and E. Abrahams, Phys. Rev. B **76**, 180501(R) (2007).
[22] Following Ref. 18, we have chosen a specific form for γ: $\gamma(T) = \gamma(T_c)(T/T_c)^3$ for $T \leq T_c$ and $\gamma(T) = \gamma(T_c)(T/T_c)$ for $T > T_c$.
[23] Here, $\xi_{\mathbf{k}} = -2t(\cos k_x + \cos k_y) - 4t' \cos k_x \cos k_y - \mu$ is the normal-state tight-binding dispersion with $t = 300$ meV, $t'/t = -0.4$, and $\mu(T=0)/t = -1.083$. Here, for definiteness, we take $T_c = 5.9$ meV and $\Delta(T_c) = 52$ meV, with $n = 0.85$, representing a moderately underdoped system (Ref. 24).
[24] A. G. Loeser, Z.-X. Shen, D. S. Dessau, D. S. Marshall, C. H. Park, P. Fournier, and A. Kapitulnik, Science **273**, 325 (1996).